PHYSICAL REVIEW D **85,** 091102(R) (2012)

Measurement of $B^0 \to J/\psi\eta^{(\prime)}$ and constraint on the $\eta - \eta'$ mixing angle

M.-C. Chang,[5] Y.-C. Duh,[5] J.-Y. Lin,[5] I. Adachi,[11] K. Adamczyk,[37] H. Aihara,[54] D. M. Asner,[42] T. Aushev,[18] A. M. Bakich,[48] V. Bhardwaj,[33] B. Bhuyan,[13] A. Bondar,[2] A. Bozek,[37] M. Bračko,[28,19] J. Brodzicka,[37] T. E. Browder,[10] P. Chang,[36] A. Chen,[34] K.-F. Chen,[36] P. Chen,[36] B. G. Cheon,[9] K. Chilikin,[18] R. Chistov,[18] I.-S. Cho,[60] S.-K. Choi,[8] Y. Choi,[47] J. Dalseno,[29,50] Z. Doležal,[3] Z. Drásal,[3] A. Drutskoy,[18] S. Eidelman,[2] J. E. Fast,[42] V. Gaur,[49] A. Garmash,[2] Y. M. Goh,[9] B. Golob,[26,19] J. Haba,[11] T. Hara,[11] K. Hayasaka,[32] H. Hayashii,[33] Y. Horii,[32] Y. Hoshi,[52] W.-S. Hou,[36] H. J. Hyun,[24] T. Iijima,[32,31] A. Ishikawa,[53] R. Itoh,[11] M. Iwabuchi,[60] Y. Iwasaki,[11] T. Iwashita,[33] T. Julius,[30] N. Katayama,[11] T. Kawasaki,[39] H. O. Kim,[24] J. B. Kim,[23] K. T. Kim,[23] M. J. Kim,[24] Y. J. Kim,[22] K. Kinoshita,[4] B. R. Ko,[23] S. Koblitz,[29] P. Kodyš,[3] S. Korpar,[28,19] P. Križan,[26,19] P. Krokovny,[2] T. Kuhr,[21] R. Kumar,[43] T. Kumita,[56] Y.-J. Kwon,[60] J. S. Lange,[6] S.-H. Lee,[23] J. Li,[46] Y. Li,[58] J. Libby,[14] C. Liu,[45] Z. Q. Liu,[15] R. Louvot,[25] S. McOnie,[48] K. Miyabayashi,[33] H. Miyata,[39] Y. Miyazaki,[31] R. Mizuk,[18] G. B. Mohanty,[49] A. Moll,[29,50] N. Muramatsu,[44] Y. Nagasaka,[12] I. Nakamura,[11] E. Nakano,[41] M. Nakao,[11] H. Nakazawa,[34] Z. Natkaniec,[37] S. Nishida,[11] K. Nishimura,[10] O. Nitoh,[57] S. Ogawa,[51] T. Ohshima,[31] S. Okuno,[20] S. L. Olsen,[46] G. Pakhlova,[18] C. W. Park,[47] K. S. Park,[47] T. K. Pedlar,[27] T. Peng,[45] R. Pestotnik,[19] M. Petrič,[19] L. E. Piilonen,[58] M. Röhrken,[21] S. Ryu,[46] H. Sahoo,[10] K. Sakai,[11] Y. Sakai,[11] O. Schneider,[25] C. Schwanda,[16] A. J. Schwartz,[4] K. Senyo,[59] M. E. Sevior,[30] M. Shapkin,[17] C. P. Shen,[31] T.-A. Shibata,[55] J.-G. Shiu,[36] A. Sibidanov,[48] F. Simon,[29,50] P. Smerkol,[19] Y.-S. Sohn,[60] A. Sokolov,[17] E. Solovieva,[18] S. Stanič,[40] M. Starič,[19] M. Sumihama,[7] T. Sumiyoshi,[56] S. Tanaka,[11] G. Tatishvili,[42] Y. Teramoto,[41] M. Uchida,[55] S. Uehara,[11] T. Uglov,[18] Y. Unno,[9] S. Uno,[11] P. Urquijo,[1] Y. Usov,[2] G. Varner,[10] V. Vorobyev,[2] C. H. Wang,[35] M.-Z. Wang,[36] P. Wang,[15] Y. Watanabe,[20] K. M. Williams,[58] E. Won,[23] H. Yamamoto,[53] Y. Yamashita,[38] C. Z. Yuan,[15] Y. Yusa,[39] Z. P. Zhang,[45] V. Zhilich,[2] V. Zhulanov,[2] and A. Zupanc[21]

[1]*University of Bonn, Bonn*
[2]*Budker Institute of Nuclear Physics SB RAS and Novosibirsk State University, Novosibirsk 630090*
[3]*Faculty of Mathematics and Physics, Charles University, Prague*
[4]*University of Cincinnati, Cincinnati, Ohio 45221*
[5]*Department of Physics, Fu Jen Catholic University, Taipei*
[6]*Justus-Liebig-Universität Gießen, Gießen*
[7]*Gifu University, Gifu*
[8]*Gyeongsang National University, Chinju*
[9]*Hanyang University, Seoul*
[10]*University of Hawaii, Honolulu, Hawaii 96822*
[11]*High Energy Accelerator Research Organization (KEK), Tsukuba*
[12]*Hiroshima Institute of Technology, Hiroshima*
[13]*Indian Institute of Technology Guwahati, Guwahati*
[14]*Indian Institute of Technology Madras, Madras*
[15]*Institute of High Energy Physics, Chinese Academy of Sciences, Beijing*
[16]*Institute of High Energy Physics, Vienna*
[17]*Institute of High Energy Physics, Protvino*
[18]*Institute for Theoretical and Experimental Physics, Moscow*
[19]*J. Stefan Institute, Ljubljana*
[20]*Kanagawa University, Yokohama*
[21]*Institut für Experimentelle Kernphysik, Karlsruher Institut für Technologie, Karlsruhe*
[22]*Korea Institute of Science and Technology Information, Daejeon*
[23]*Korea University, Seoul*
[24]*Kyungpook National University, Taegu*
[25]*École Polytechnique Fédérale de Lausanne (EPFL), Lausanne*
[26]*Faculty of Mathematics and Physics, University of Ljubljana, Ljubljana*
[27]*Luther College, Decorah, Iowa 52101*
[28]*University of Maribor, Maribor*
[29]*Max-Planck-Institut für Physik, München*
[30]*University of Melbourne, School of Physics, Victoria 3010*
[31]*Graduate School of Science, Nagoya University, Nagoya*
[32]*Kobayashi-Maskawa Institute, Nagoya University, Nagoya*
[33]*Nara Women's University, Nara*
[34]*National Central University, Chung-li*
[35]*National United University, Miao Li*
[36]*Department of Physics, National Taiwan University, Taipei*

[37]*H. Niewodniczanski Institute of Nuclear Physics, Krakow*
[38]*Nippon Dental University, Niigata*
[39]*Niigata University, Niigata*
[40]*University of Nova Gorica, Nova Gorica*
[41]*Osaka City University, Osaka*
[42]*Pacific Northwest National Laboratory, Richland, Washington 99352*
[43]*Panjab University, Chandigarh*
[44]*Research Center for Nuclear Physics, Osaka University, Osaka*
[45]*University of Science and Technology of China, Hefei*
[46]*Seoul National University, Seoul*
[47]*Sungkyunkwan University, Suwon*
[48]*School of Physics, University of Sydney, NSW 2006*
[49]*Tata Institute of Fundamental Research, Mumbai*
[50]*Excellence Cluster Universe, Technische Universität München, Garching*
[51]*Toho University, Funabashi*
[52]*Tohoku Gakuin University, Tagajo*
[53]*Tohoku University, Sendai*
[54]*Department of Physics, University of Tokyo, Tokyo*
[55]*Tokyo Institute of Technology, Tokyo*
[56]*Tokyo Metropolitan University, Tokyo*
[57]*Tokyo University of Agriculture and Technology, Tokyo*
[58]*CNP, Virginia Polytechnic Institute and State University, Blacksburg, Virginia 24061*
[59]*Yamagata University, Yamagata*
[60]*Yonsei University, Seoul*

(Received 15 March 2012; published 4 May 2012)

We measure the branching fractions of $B^0 \to J/\psi\,\eta^{(\prime)}$ decays with the complete Belle data sample of 772×10^6 $B\bar{B}$ events collected at the $\Upsilon(4S)$ resonance with the Belle detector at the KEKB asymmetric-energy e^+e^- collider. The results for the branching fractions are: $\mathcal{B}(B^0 \to J/\psi\,\eta) = (12.3\,^{+1.8}_{-1.7} \pm 0.7) \times 10^{-6}$ and $\mathcal{B}(B^0 \to J/\psi\,\eta') < 7.4 \times 10^{-6}$ at 90% confidence level. The η-η' mixing angle is constrained to be less than 42.2° at 90% confidence level.

DOI: 10.1103/PhysRevD.85.091102 PACS numbers: 13.20.Gd, 13.20.He, 13.25.Hw, 14.40.Nd

The neutral B meson decays $B^0 \to J/\psi\,\eta^{(\prime)}$ are mediated by the $\bar{b} \to c\bar{c}\,\bar{d}$ transition as shown in Fig. 1. For such final states involving an η or η' meson, it is convenient to consider flavor mixing of η_q and η_s defined by

$$\eta_q = \frac{1}{\sqrt{2}}(u\bar{u} + d\bar{d}), \qquad \eta_s = s\bar{s}, \tag{1}$$

in analogy with the wave functions of ω and ϕ for ideal mixing [1]. The wave functions of the η and η' are given by

$$\begin{pmatrix} \eta \\ \eta' \end{pmatrix} = \begin{pmatrix} \cos\phi & -\sin\phi \\ \sin\phi & \cos\phi \end{pmatrix} \begin{pmatrix} \eta_q \\ \eta_s \end{pmatrix}. \tag{2}$$

If the $s\bar{s}$ component in Eq. (2) for $B^0 \to J/\psi\,\eta^{(\prime)}$ decays is negligible, the branching fractions are related to the η-η' mixing angle ϕ as

$$\frac{\mathcal{B}(B^0 \to J/\psi\,\eta')}{\mathcal{B}(B^0 \to J/\psi\,\eta)} \simeq \tan^2\phi. \tag{3}$$

Using the measured values of the η-η' mixing angle $\phi \sim 40°$ [2] and $\mathcal{B}(B^0 \to J/\psi\,\eta) = (9.5 \pm 1.7 \pm 0.8) \times 10^{-6}$ [3] in Eq. (3), the expected branching fraction for $B^0 \to J/\psi\,\eta'$ is about 6.7×10^{-6}. Other predictions give $\mathcal{B}(B^0 \to J/\psi\,\eta') = (4 - 8) \times 10^{-6}$ and η-η' mixing angle $37° < \phi < 50°$ [4–7]. Recently, $B_s^0 \to J/\psi\,\eta^{(\prime)}$ decays have been observed by Belle [8]. The branching fractions in Ref. [8] and this paper provide good inputs for model predictions [4–7]. The existing upper limit for the $B^0 \to J/\psi\,\eta'$ branching fraction is 6.3×10^{-5} [9].

In this paper, we report a measurement of $B^0 \to J/\psi\,\eta$ and a search for $B^0 \to J/\psi\,\eta'$ decays [10]. The results are based on a data sample that contains 772×10^6 $B\bar{B}$ pairs, collected with the Belle detector at the KEKB asymmetric-energy e^+e^- (3.5 on 8 GeV) collider [11] operating at the $\Upsilon(4S)$ resonance.

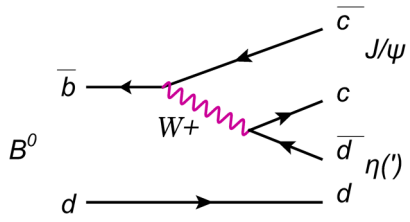

FIG. 1 (color online). Quark-level diagram of the leading transition $B^0 \to J/\psi\,\eta^{(\prime)}$.

The Belle detector is a large-solid-angle magnetic spectrometer that consists of a silicon vertex detector (SVD), a 50-layer central drift chamber (CDC), an array of aerogel threshold Cherenkov counters (ACC), a barrel-like arrangement of time-of-flight scintillation counters (TOF), and an electromagnetic calorimeter (ECL) located inside a superconducting solenoid coil that provides a 1.5 T magnetic field. An iron flux-return located outside of the coil is instrumented to detect K_L^0 mesons and to identify muons (KLM). The detector is described in detail elsewhere [12].

The data sample used in this analysis was collected with two detector configurations. A 2.0 cm beampipe and a 3-layer silicon vertex detector were used for the first sample of $152 \times 10^6 B\bar{B}$ pairs, while a 1.5 cm beampipe, a 4-layer silicon detector, and a small-cell inner drift chamber were used to record the remaining $620 \times 10^6 B\bar{B}$ pairs [13]. GEANT-based Monte Carlo(MC) simulation program is used to model the response of the detector and to determine the reconstruction efficiencies. Simulated events are generated with the EvtGen program [14], except for the $B^0 \to J/\psi\eta'(\eta' \to \rho^0\gamma)$ mode for which we use the QQ program [15] since EvtGen does not properly generate the ρ^0 mass and angular distributions.

Charged tracks are selected by using the impact parameters relative to the interaction point: dr for the radial direction and dz for the direction along the positron beam. Our requirements are $dr < 1$ cm and $|dz| < 5$ cm. Identification of e^+ and e^- from J/ψ decay uses information from the ECL, the CDC (dE/dx), and the ACC. Identification of μ^+ and μ^- candidates uses a track penetration depth and hit pattern in the KLM system. Charged pions are identified based on the information from the CDC (dE/dx), the TOF, and the ACC.

Photon candidates are selected from showers in the ECL, which are not associated with charged tracks, and an energy deposition of at least 50 MeV in the barrel region or 100 MeV in the end-cap region. A pair of photons with an invariant mass in the range $117.8\ \mathrm{MeV}/c^2 < M_{\gamma\gamma} < 150.2\ \mathrm{MeV}/c^2$ is considered as a π^0 candidate. This invariant mass region corresponds to a $\pm 3\sigma$ interval around the π^0 mass, where σ is the mass resolution.

We reconstruct J/ψ mesons in the l^+l^- decay channel ($l = e$ or μ). Any photon within 50 mrad of e^+ or e^- tracks is included as well. The invariant mass is required to be within $-0.15\,\mathrm{GeV}/c^2 < M_{ee(\gamma)} - m_{J/\psi} < 0.036\,\mathrm{GeV}/c^2$ and $-0.06\ \mathrm{GeV}/c^2 < M_{\mu\mu} - m_{J/\psi} < 0.036\ \mathrm{GeV}/c^2$, where $m_{J/\psi}$ denotes the nominal J/ψ mass [16], $M_{ee(\gamma)}$ and $M_{\mu\mu}$ are the reconstructed invariant mass of $e^+e^-(\gamma)$ and $\mu^+\mu^-$, respectively. An asymmetric interval is used to include part of the radiative tails.

η mesons are reconstructed in the $\gamma\gamma$ and $\pi^+\pi^-\pi^0$ final states. The mass ranges are $497\ \mathrm{MeV}/c^2 < M_{\gamma\gamma} < 590\ \mathrm{MeV}/c^2$ and $520\,\mathrm{MeV}/c^2 < M_{\pi^+\pi^-\pi^0} < 557\,\mathrm{MeV}/c^2$. In the $\gamma\gamma$ final state, candidates in which either of the daughter photons forms a π^0 together with any other photon in the event are rejected. In the $\gamma\gamma$ final state, we require $|\cos\theta_\eta| < 0.9$, where θ_η is defined as the angle between the momentum of either of the photons and the boost direction of the laboratory system in the rest frame of the η.

η' mesons are reconstructed in the $\eta\pi^+\pi^-$ ($\eta \to \gamma\gamma$) and $\rho^0\gamma$ final states. The mass ranges are $930\ \mathrm{MeV}/c^2 < M_{\eta\pi^+\pi^-} < 967\ \mathrm{MeV}/c^2$, $920\ \mathrm{MeV}/c^2 < M_{\rho^0\gamma} < 980\ \mathrm{MeV}/c^2$, and $600\ \mathrm{MeV}/c^2 < M_{\rho^0} < 900\ \mathrm{MeV}/c^2$. In the $\rho^0\gamma$ final state, we require $\cos\theta_{\eta'} < 0.6$ and $|\cos\theta_\rho| < 0.8$. Here $\theta_{\eta'}$ is the angle between the photon momentum and the opposite of the boost direction of the laboratory system in the η' rest frame. The other angle, θ_ρ, is the angle between the π^+ momentum and the boost direction of the laboratory system in the ρ rest frame.

B mesons are reconstructed in the $J/\psi\eta^{(\prime)}$ final state. Signal candidates are identified using two kinematic variables defined in the $\Upsilon(4S)$ center-of-mass (CM) frame: the beam-energy constrained mass, $M_{\mathrm{bc}} = \sqrt{E_{\mathrm{beam}}^2 - p_B^{*2}}$ and the energy difference, $\Delta E = E_B^* - E_{\mathrm{beam}}$, where p_B^* and E_B^* are the momentum and energy of the B candidate and E_{beam} is the run-dependent beam energy [17]. To improve the momentum resolution, the masses of the selected π^0, $\eta^{(\prime)}$ and J/ψ candidates are constrained to their nominal masses using mass-constrained kinematic fits. In addition, vertex-constrained fits are applied to $\eta \to \pi^+\pi^-\pi^0$, $\eta' \to \eta\pi^+\pi^-$ and $J/\psi \to l^+l^-$ candidates. We retain events with $M_{\mathrm{bc}} > 5.2\ \mathrm{GeV}/c^2$ and $|\Delta E| < 0.2$ GeV. The signal peaks in the region defined by $5.27\ \mathrm{GeV}/c^2 < M_{\mathrm{bc}} < 5.29\ \mathrm{GeV}/c^2$, $|\Delta E| < 0.05$ GeV [or $-0.10\ \mathrm{GeV} < \Delta E < 0.05$ GeV for $B^0 \to J/\psi\eta(\eta \to \gamma\gamma)$ only].

For events with more than one B candidate, which are usually due to multiple $\eta^{(\prime)}$ candidates, the candidate with the minimum χ^2 value from the mass- and vertex-constrained fit is chosen.

The combinatorial background dominated by two-jet-like $e^+e^- \to q\bar{q}(q = u, d, s, c)$ continuum is suppressed by requiring the ratio of second to zeroth Fox-Wolfram moments $R_2 < 0.4$ [18].

After the continuum suppression, the background is dominated by $B\bar{B}$ events with $B \to J/\psi X$ decays, where X denotes any final state. Using an MC sample of generic $B\bar{B}$ decays corresponding to 10 times larger than the data, with all known and expected $B^0 \to J/\psi X$ decays, we study these backgrounds. The backgrounds from $B^0 \to J/\psi K$ and $B^0 \to J/\psi\pi^0$ cannot be highly suppressed and peak in the M_{bc} distributions but not in ΔE.

A figure-of-merit (FOM) method is used to optimize the selection requirements. The maximal value of $N_s/\sqrt{N_s + N_b}$ is chosen for each variable, where N_s is the number of expected signal events and N_b is the number of background events.

For each requirement, N_s is estimated from signal MC simulation as

$$N_s = N_{B\bar{B}}\mathcal{B}(B^0 \to J/\psi\eta')\varepsilon\mathcal{B}_{\rm sec}, \quad (4)$$

where $N_{B\bar{B}}$ is the total number of $B\bar{B}$ pairs, 6.7×10^{-6} is assumed for $\mathcal{B}(B^0 \to J/\psi\eta')$, ε is the signal efficiency, and $\mathcal{B}_{\rm sec}$ is a product of the branching fractions for secondary decays.

The value of N_b is estimated from

$$N_b = R_{\rm MC}N_b', \quad (5)$$

where $R_{\rm MC}$ is the fraction of $B \to J/\psi X$ MC events in the signal region, and N_b' is the number of data events in the ΔE sideband region.

Signal yields and background levels are determined by fitting the ΔE distribution for candidates in the $M_{\rm bc}$ signal region. For $B^0 \to J/\psi\eta$, the ΔE distribution is fitted using a signal probability density function (PDF), which is a sum of a Crystal Ball function [19] and two Gaussian functions. For $B^0 \to J/\psi\eta'$, the signal PDF is a sum of three Gaussian functions. The two signal PDFs are chosen based on fits to large MC samples. For the background we use a second-order polynomial function with floating coefficients.

We use the $B^+ \to J/\psi K^{*+}(K^{*+} \to K^+\pi^0)$ decay as a control sample to correct the difference between data and MC in the fitted mean and width of the ΔE signal peak. We require the helicity angle θ_{K^*} in the $K^{*+} \to K^+\pi^0$ decay to be less than 90 degrees. Here θ_{K^*} is the angle between the π^0 momentum and the opposite of the boost direction of the laboratory system in the K^{*+} rest frame. This requirement primarily selects events with a high momentum π^0 and produces a control-sample ΔE distribution that is similar to that in our decay.

The signal PDFs are modified based on the differences of mean and width between data and MC in the control sample. From a fit to the control sample, we find that the mean values are shifted by (-3.85 ± 0.13) MeV. The width in data is (1.11 ± 0.03) times wider than in MC simulation.

We determine the signal yields by performing an unbinned extended maximum-likelihood fit to the candidate data events,

$$\mathcal{L} = \frac{e^{-(N_s+N_b)}}{N}\prod_i^N [N_s P_s(\Delta E_i) + N_b P_b(\Delta E_i)]. \quad (6)$$

Here N is the total number of candidate events, $P_s(\Delta E_i)$ and $P_b(\Delta E_i)$ denote the signal and background ΔE PDFs, respectively, and i is the event index.

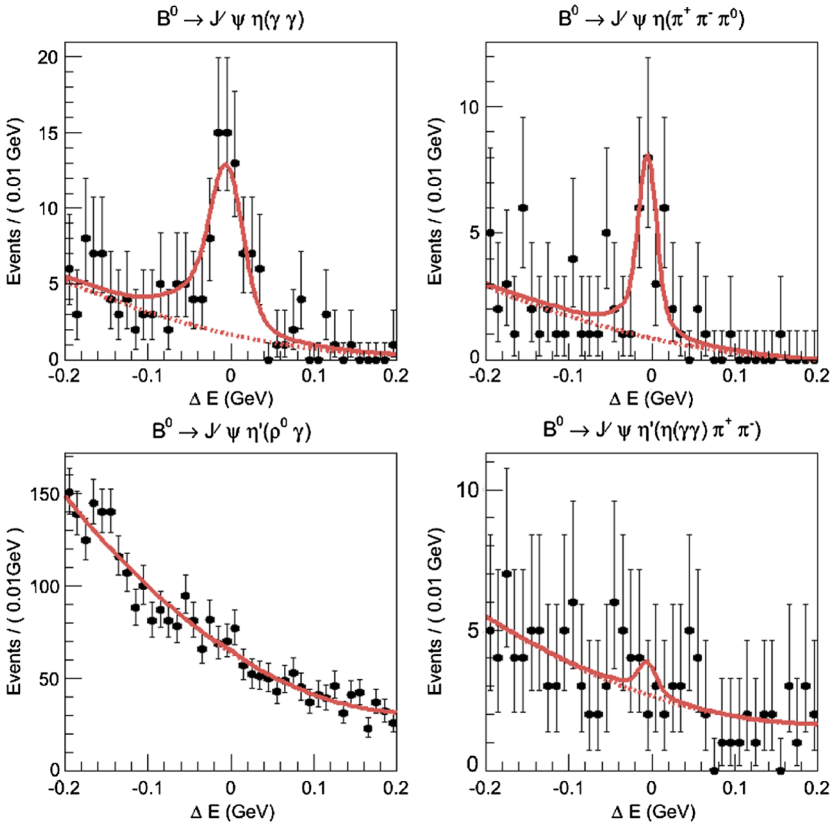

FIG. 2 (color online). ΔE distributions for the two decay modes, $B^0 \to J/\psi\eta$ and $B^0 \to J/\psi\eta'$. The plots on the top are $B^0 \to J/\psi\eta$, in the left-hand side—$B^0 \to J/\psi\eta(\eta \to \gamma\gamma)$, in the right-hand side—$B^0 \to J/\psi\eta(\eta \to \pi^+\pi^-\pi^0)$. The plots on the bottom are $B^0 \to J/\psi\eta'$, in the left-hand side—$B^0 \to J/\psi\eta'(\eta' \to \rho^0\gamma)$, in the right-hand side—$B^0 \to J/\psi\eta'(\eta' \to \eta\pi^+\pi^-)$. The solid curves are results of the overall fit while the dashed curves are the background shapes.

In the $B^0 \to J/\psi\eta$ mode, we fit the $B^0 \to J/\psi\eta(\gamma\gamma)$ and $B^0 \to J/\psi\eta(\pi^+\pi^-\pi^0)$ candidate samples simultaneously with a common branching fraction. The fit gives the branching fraction $(12.3 \pm^{1.8}_{1.7}) \times 10^{-6}$, which corresponds to signal yields of $(77.9 \pm^{11.4}_{10.8})$ and $(29.8 \pm^{4.4}_{4.1})$ for the $\eta(\gamma\gamma)$ and $\eta(\pi^+\pi^-\pi^0)$ modes, respectively. For the $B^0 \to J/\psi\eta'$ mode, we also fit the $B^0 \to J/\psi\eta'(\eta\pi^+\pi^-)$ and $B^0 \to J/\psi\eta'(\rho^0\gamma)$ candidate samples simultaneously with a common branching fraction. The fit gives the branching fraction $(2.2 \pm^{3.3}_{2.9}) \times 10^{-6}$, which corresponds to signal yields of $(5.5 \pm^{8.3}_{7.2})$ and $(5.2 \pm^{7.8}_{6.9})$ for the $\eta'(\rho^0\gamma)$ and $\eta'(\eta\pi^+\pi^-)$ modes, respectively. The results of the fits to the data are shown in Fig. 2.

A 1.4% systematic error comes from the uncertainty in the number of $B\bar{B}$ pairs. The systematic error due to tracking is 0.35% for each charged track. The systematic error from the pion identification requirement is determined from a study of the $D^{*+} \to D^0\pi^+(D^0 \to K^-\pi^+)$ control sample. The systematic error from lepton identification is obtained from a comparison between the data and MC for $\gamma\gamma \to e^+e^-/\mu^+\mu^-$ events.

A 3.0% systematic error due to π^0 detection is determined from a comparison of the data and MC ratios for a large sample of $\eta \to \pi^+\pi^-\pi^0$ and $\eta \to 3\pi^0$ decays. Since $\eta \to \gamma\gamma$ is similar to π^0 decay, we also assign a 3.0% systematic error for $\eta \to \gamma\gamma$ reconstruction.

We use the previously mentioned control sample $B^+ \to J/\psi K^{*+}(K^{*+} \to K^+\pi^0)$ to obtain the systematic errors from the $R_2 < 0.4$ requirement and signal PDFs. A 3.3% systematic error is obtained by comparing the data and MC. The systematic errors from the signal and background PDFs are obtained by comparing the fit results for the cases when the fitting parameters are fixed from either MC or data and from changes that result from varying each parameter by one standard deviation. The errors on the branching fractions are taken from Ref. [16].

The systematic errors are summarized in Tables I and II. The total uncertainty is calculated by summing all individual uncertainties in quadrature.

TABLE I. Systematic uncertainties for $B \to J/\psi\eta$ (%). The combined systematic error is 5.9%.

η source	$\gamma\gamma$	$\pi^+\pi^-\pi^0$
Number of events $B\bar{B}$ events	1.4	1.4
Tracking	0.7	1.4
Lepton-ID	2.6	2.6
Charged π-ID	-	2.4
$\eta \to \gamma\gamma$, π^0 selection	3.0	3.0
PDFs	1.3	1.3
$R_2 < 0.4$	3.3	3.3
$\mathcal{B}(J/\psi \to e^+e^-, \mu^+\mu^-)$	1.0	1.0
$\mathcal{B}(\eta \to \gamma\gamma)$	0.5	-
$\mathcal{B}(\eta \to \pi^+\pi^-\pi^0)$	-	1.2
Total	5.7	6.4

TABLE II. Systematic uncertainties for $B \to J/\psi\eta'$ (%). The combined systematic error is 7.5%.

η' source	$\eta\pi^+\pi^-$	$\rho^0\gamma$
Number of $B\bar{B}$ events	1.4	1.4
Tracking (lepton and charged pion)	1.4	1.4
Lepton-ID	2.6	2.6
Charged π-ID	3.0	3.0
$\eta \to \gamma\gamma$, π^0 selection	3.0	3.0
PDFs	3.6	3.6
$R_2 < 0.4$	3.3	3.3
$\mathcal{B}(J/\psi \to e^+e^-, \mu^+\mu^-)$	1.0	1.0
$\mathcal{B}(\eta \to \gamma\gamma)$	0.5	-
$\mathcal{B}(\eta' \to \rho^0\gamma)$	-	2.0
$\mathcal{B}(\eta' \to \eta\pi^+\pi^-)$	1.6	-
Total	7.5	7.6

The statistical significances of the observed $B^0 \to J/\psi\eta$ and $B^0 \to J/\psi\eta'$ yields are 6.3σ and 0.4σ, respectively. The significance is defined as $\sqrt{-2\ln(L_0/L_{\max})}$, where $L_{\max}(L_0)$ denotes the likelihood value at the maximum (with the signal yield fixed at zero). The systematic errors associated with the choice of signal and background PDFs are included in the significance calculation.

An upper limit has been evaluated for the branching fraction of $B^0 \to J/\psi\eta'$ at 90% confidence level because of the low significance. The Bayesian upper limits are obtained from

$$\int_0^N L(n)dn = 0.9 \int_0^\infty L(n)dn, \tag{7}$$

where N denotes the signal yield. We use a modified likelihood function to obtain a conservative upper limit, which is smeared with the systematic errors in the branching fraction. The upper limit for the branching fraction of $B^0 \to J/\psi\eta'$ at 90% confidence level is 7.4×10^{-6}.

The signal efficiencies and the branching fractions are listed in Table III.

In summary, we measure the branching fraction $\mathcal{B}(B^0 \to J/\psi\eta) = (12.3 \pm^{1.8}_{1.7} \pm 0.7) \times 10^{-6}$. The first error is statistical and the second is systematic. This result is consistent with and supersedes the previous Belle measurement [3]. We do not observe a significant signal in $B^0 \to J/\psi\eta'$

TABLE III. MC efficiencies and branching fractions.

Mode	MC Efficiency (%)	$\mathcal{B}(10^{-6})$
$B^0 \to J/\psi\eta(\gamma\gamma)$	35.7	
$B^0 \to J/\psi\eta(\pi^+\pi^-\pi^0)$	24.6	
$B^0 \to J/\psi\eta$ combined		$12.3 \pm^{1.8}_{1.7} \pm 0.7$
$B^0 \to J/\psi\eta'(\eta\pi^+\pi^-)$	31.0	
$B^0 \to J/\psi\eta'(\rho^0\gamma)$	19.1	
$B^0 \to J/\psi\eta'$ combined		$2.2 \pm^{3.3}_{2.9} \pm 0.2$
$B^0 \to J/\psi\eta'$ UL (90%)		<7.4

and set the upper limit $\mathcal{B}(B^0 \to J/\psi\eta') < 7.4 \times 10^{-6}$ at 90% confidence level, which is eight times more stringent than the previous result [9]. From Eq. (3) we calculate the η-η' mixing angle, which is less than 42.2° at 90% confidence level. These results are consistent with the theoretical predictions of Refs. [4–7].

We thank the KEKB group for the excellent operation of the accelerator; the KEK cryogenics group for the efficient operation of the solenoid; and the KEK computer group, the National Institute of Informatics, and the PNNL/EMSL computing group for valuable computing and SINET4 network support. We acknowledge support from the Ministry of Education, Culture, Sports, Science, and Technology (MEXT) of Japan, the Japan Society for the Promotion of Science (JSPS), and the Tau-Lepton Physics Research Center of Nagoya University; the Australian Research Council and the Australian Department of Industry, Innovation, Science and Research; the National Natural Science Foundation of China under contract Nos. 10575109, 10775142, 10875115, and 10825524; the Ministry of Education, Youth and Sports of the Czech Republic under Contract No. LA10033 and MSM0021620859; the Department of Science and Technology of India; the Istituto Nazionale di Fisica Nucleare of Italy; the BK21 and WCU program of the Ministry Education Science and Technology, National Research Foundation of Korea, and GSDC of the Korea Institute of Science and Technology Information; the Polish Ministry of Science and Higher Education; the Ministry of Education and Science of the Russian Federation, and the Russian Federal Agency for Atomic Energy; the Slovenian Research Agency; the Swiss National Science Foundation; the National Science Council and the Ministry of Education of Taiwan; and the U.S. Department of Energy and the National Science Foundation. This work is supported by a Grant-in-Aid from MEXT for Science Research in a Priority Area (''New Development of Flavor Physics''), and from JSPS for Creative Scientific Research (''Evolution of Tau-lepton Physics'').

[1] H.-Y. Cheng and C.-W. Chiang, Phys. Rev. D **81**, 074021 (2010).
[2] F. Ambrosino *et al.*, J. High Energy Phys. 07 (2009) 105.
[3] M.-C. Chang *et al.* (Belle Collaboration), Phys. Rev. Lett. **98**, 131803 (2007).
[4] J.-W. Li and D.-S. Du, Phys. Rev. D **78**, 074030 (2008).
[5] C. E. Thomas, J. High Energy Phys. 10 (2007) 026.
[6] T. Feldmann, P. Kroll, and B. Stech, Phys. Rev. D **58**, 114006 (1998); Phys. Lett. B **449**, 339 (1999).
[7] R. Fleischer, R. Knegjens, and G. Ricciardi, Eur. Phys. J. C **71**, 1798 (2011).
[8] J. Li *et al.* (Belle Collaboration), arXiv:1202.0103.
[9] B. Aubert *et al.* (*BABAR* Collaboration), Phys. Rev. Lett. **91**, 071801 (2003).
[10] Throughout this paper, the inclusion of the charge-conjugate decay mode is implied unless otherwise stated.
[11] S. Kurokawa and E. Kikutani, Nucl. Instrum. Methods Phys. Res., Sect. A **499**, 1 (2003), and other papers included in this volume.
[12] A. Abashian *et al.* (Belle Collaboration), Nucl. Instrum. Methods Phys. Res., Sect. A **479**, 117 (2002).
[13] Z. Natkaniec *et al.* (Belle SVD2 Group), Nucl. Instrum. Methods Phys. Res., Sect. A **560**, 1 (2006).
[14] D. J. Lange, Nucl. Instrum. Methods Phys. Res., Sect. A **462**, 152 (2001). (see http://www.slac.stanford.edu/lange/EvtGen)
[15] Events are generated with the CLEO QQ generator (see http://www.lns.cornell.edu/public/CLEO/soft/QQ)
[16] K. Nakamura *et al.* (Particle Data Group), J. Phys. G **37**, 075021 (2010) and 2011 partial update to the 2012 edition.
[17] Since beam conditions vary slightly for different running periods, we use the run-dependent beam energy to preserve the precision of the $M_{\rm bc}$ and ΔE determinations.
[18] The Fox-Wolfram moments were introduced in G. C. Fox and S. Wolfram, Phys. Rev. Lett. **41**, 1581 (1978).
[19] T. Skwarnicki, Ph.D. thesis, Institute for Nuclear Physics, Krakow 1986; DESY Internal Report, Report No. DESY F31-86-02, 1986.